

Subcritical growth of long cracks in heterogeneous ceramics

N. ESWARA PRASAD, S. B. BHADURI

Defence Metallurgical Research Laboratory, Hyderabad 500 258, India

This paper models subcritical growth of long cracks in ceramic structures containing heterogeneities. In such cases, the microstructure is believed to promote deflection of the crack. Due to this, the following effects are observed: (1) there is scatter in K_I - V data; (2) N , the subcritical crack growth susceptibility coefficient, as obtained from specimens with long cracks, has an erroneously large value as compared to specimens with small flaws; and (3) life time predicted from long crack experiments (especially in the double torsion load relaxation mode) is more than the predictions from short cracks. All of these effects, as mentioned above, are explained by the present model.

1. Introduction

The subcritical crack-growth phenomenon in brittle ceramics is a handicap for their use as a structural material. Because of the subcritical crack growth, the material may fail months after the first application of the load. Usually three kinds of test are carried out to understand this slow crack growth behaviour [1]. The first type of crack growth test uses fracture mechanics samples containing large cracks. In such tests, crack growth rates, V , are measured *vis-à-vis* the applied stress intensity factor, K_I , thereby generating the so-called K_I - V curve. It is generally assumed that the crack growth velocity, V , and the applied stress intensity factor, K_I , have a power law relationship as shown in Equation 1

$$V = A(K_I)^N \quad (1)$$

where A and N are constants. N is known as the subcritical crack growth susceptibility coefficient. The extent of subcritical crack growth is large in materials having small values of N and vice versa. In the second kind of test, samples (either containing indentation cracks or machining flaws) are fractured using various constant stressing rates. It has been shown [1] that an estimate of N can be obtained from the above data. Information obtained from both of these tests can lead to predictions of life time of the structure in question. In the third kind of test, specimens are stressed under dead weight load, and time to fracture is noted. Although this test directly produces the life time data, carrying it out is difficult because of the long times taken in some cases. Therefore, the first two types of tests are often employed in calculating life times. These tests are performed assuming that crack-growth parameters are independent of the specimen geometry and microstructure. However, it has been shown by Pletka and Wiederhorn [2, 3] that the above assumptions do not hold good for heterogeneous structures. Values of N determined from specimens having large cracks are significantly higher than those evaluated from specimens with short cracks. It is

believed that this effect is a manifestation of the microstructure. So microstructure and specimen geometry are actually inter-related. Long cracks, which are longer than the scale of microstructure obviously have a different growth behaviour compared to the short cracks, which are of the same size to the scale of microstructure. Therefore, attention must be paid to the crack paths in the experimental samples during crack growth testing.

This question was re-examined by Cook and co-workers [4, 5] by performing very elegant indentation tests. They varied the indentation load to produce crack sizes which are comparable to the scale of microstructure and greater than that. Thus, variation of indentation load produced cracks in short and long crack length regimes. The data showed that as the indentation load is increased, the toughness increases finally reaching a constant value. This behaviour was rationalized in terms of a grain-localized apparent R -curve function [4, 6]. Furthermore, stressing rate tests (second kind) were carried out to check what effect the R -curve has on the subcritical crack-growth behaviour. The results show that in stressing rate experiments, long and short cracks give rise to similar N values.

Okada and Sines [7] examined the path of crack growth in the case of a delayed failure test (third kind). By careful usage of a dye penetrant, they identified that failure takes place due to growth and coalescence of very small flaws. Based on these experimental observations, they proposed a model of coalescence of cracks to predict the delayed failure of the material. The model described by Okada and Sines [7], can also lead to the explanation of scatter seen in K_I - V data observed in polycrystalline materials such as glass ceramics and PZT [8, 9].

So far, little has been reported in the literature concerning the crack paths during the subcritical growth of long cracks in ceramic samples. Pletka and Wiederhorn [3] presented micrographs of crack paths in different ceramic systems. It is evident from their micrographs that the crack path is not straight, but

TABLE I Comparison of salient features of the present paper with previous references

Sample and testing conditions	Present work	Cook <i>et al.</i> [4, 5]	Okada and Sines [7]
1. Type of experiment	Long cracks with load relaxation technique (first kind)	Stressing rate (second kind)	Dead weight loading (third kind)
2. Crack size	Long cracks only	Range of cracks both long and short	Short cracks
3. Crack path geometry	considered	Not considered	considered
4. Difference in N value from long to short crack growth regime	Explains the over-estimation of N compared to short crack data	N value remains constant for the wide range of crack size	Does not consider N value

zig-zag in nature. The intent of the present paper is to present a phenomenological model which takes into account this zig-zag behaviour of the crack path and to explain the scatter in K_I-V data for various ceramic systems. We have chosen several systems, where it is believed that such a type of crack growth can occur in specimens with large cracks. The three different materials under consideration here, have a wide size range of heterogeneities.

In order to point out important differences between the present work and that of Cook *et al.* [4, 5] and Okada and Sines [7], we have compared them in Table I. The present paper considers crack growth behaviour in specimens with long cracks (first kind of test) as opposed to other references. From this view point and others listed in Table I, it seems that the present model is complementary to the other models. In order to understand subcritical crack-growth phenomenon in ceramics, all these models have to be compared.

2. The model

As the model is based on observations made by Pletka and Wiederhorn, the salient features of their findings should be pointed out. This will enable us to set the guidelines for the model. First, Pletka and Wiederhorn's data were collected using the double torsion (DT) load relaxation technique. It is generally agreed that DT is a mode I type specimen. Even though mode I loading is applied to the specimen, the microstructure promotes mixed mode crack growth at the tip. This is evident from the micrographs of alumina having different grain sizes. Secondly, it is believed that because of the zig-zag path, there is a wide scatter in the data. In fact, in alumina with an average grain size of $16\ \mu\text{m}$, it was very difficult to obtain reliable data because of the erratic crack growth [3]. Again the micrograph of the crack path will support this conjecture.

In the literature, such zig-zag crack-growth phenomena are generally called "crack deflection". Faber

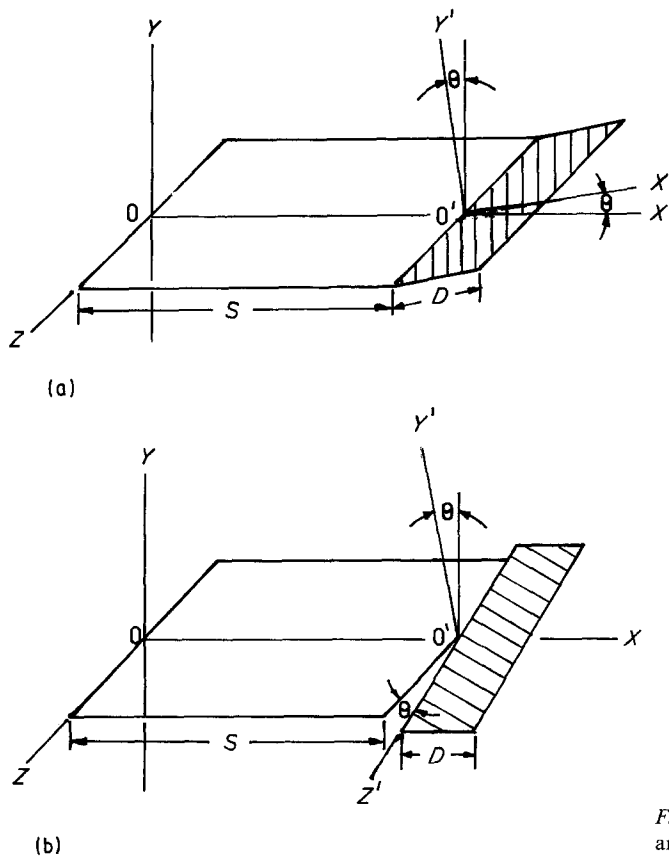


Figure 1 The two basic crack deflection mechanisms; (a) tilt mechanism, (b) twist mechanism.

and Evans [10] presented the first model to predict the increase in toughness by deflection. Suresh [11] applied the idea of crack deflection to examine fatigue crack growth in metals. We will follow his approach to treat slow crack growth in ceramics.

As discussed by Suresh [11], there could be several configurations of the deflected crack paths. The crack could be forked, kinked, twisted, etc. However, the main configurations are (1) tilted crack (Fig. 1a) and (2) twisted crack (Fig. 1b). Suresh considered crack growth by the tilting process, which is easy to model. On the other hand, Faber and Evans [10] proposed a generalized mechanism of crack deflection by tilting and twisting. To simplify the model, we will use only tilting.

Following Lawn and Wilshaw [12], we will now obtain the stress intensity factors for tilted crack. The crack is shown to be tilted about O axis at an angle θ at O', the tip of the main crack. Mode I loading is applied at O. The transformed stress intensity factors can be simply obtained by coordinate transformation from Cartesian to polar. The normal and shear components are given as:

$$\left. \begin{aligned} \sigma_{Y'Y'} &= \sigma_{\theta\theta} = \frac{K_I}{(2\pi r)^{1/2}} \cos^3 \theta/2 \\ \sigma_{XY'} &= \sigma_{r\theta} = \frac{K_I}{(2\pi r)^{1/2}} \sin \theta/2 \cos^2 \theta/2 \\ \sigma_{XZ} &= 0 \end{aligned} \right\} \quad (2)$$

The transformed stress intensity factors can be written as:

$$K_I'(\theta) = K_I \cos^3 \theta/2 \quad (3)$$

and

$$K_{II}'(\theta) = K_I \sin \theta/2 \cos^2 \theta/2$$

The idealized crack path is shown in Fig. 2, where S is the length of the straight crack and D is that of the deflected crack, whereas K_I applies to crack growth in S , and effective K_I applies to crack growth in D . Assuming a simple coplanar strain energy release rate, the effective K_I can be written as $(K_I'^2 + K_{II}'^2)^{1/2}$. Hence the average stress intensity factor during crack growth is

$$\bar{K}_I = \frac{[(K_I'^2 + K_{II}'^2)^{1/2}]D + K_I S}{(D + S)} \quad (4)$$

From Equations 2 and 3

$$\bar{K}_I = \frac{K_I(D \cos^2 \theta/2 + S)}{(D + S)} \quad (5)$$

The average velocity is given by

$$\bar{V} = \left[\frac{D \cos \theta + S}{D + S} \right] V \quad (6)$$

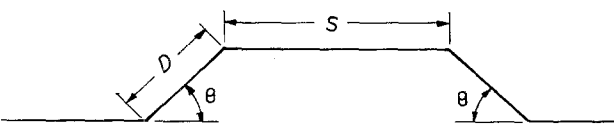


Figure 2 The geometry of a deflected crack path.

These parameters can then be plugged into typical slow crack-growth relationship

$$\bar{V} = A(\bar{K}_I)^N \quad (7)$$

where A is a constant and N is the slow crack-growth exponent. From Equations 5, 6 and 7

$$V = A \left[\frac{D \cos \theta + S}{(D + S)} \right]^{-1} \left[\frac{D \cos^2 \theta/2 + S}{(D + S)} \right]^N (K_I)^N \quad (8)$$

Note that in Equation 8, A and N are material parameters. Whereas Equation 7 is the averaged-out K_I - V relationship, Equation 8 is valid for a particular deflection condition. The average data should consist of many such deflections during the growth of the crack. These deflection conditions are defined by the ratio of $D/(D + S)$ and θ values. In this paper we judiciously choose these conditions and plot K_I - V data for a particular condition. Finally, we compare these theoretical curves to the experimentally collected data. This type of comparison shows which deflection conditions are probable in a given system.

3. Results

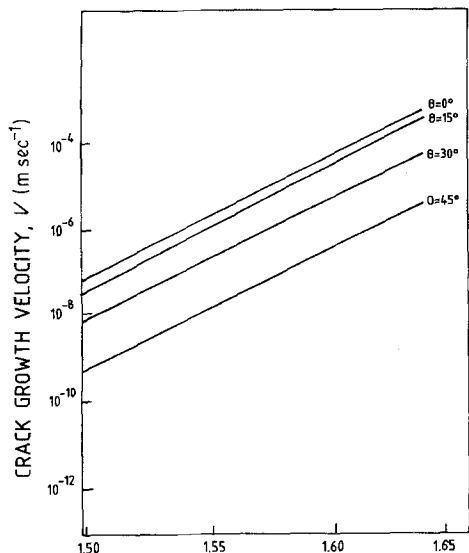
The results of this paper are based on Equation 8 and are applied to various materials. We have grouped them according to the scale of their microstructure. Cordierite-based glass ceramics which are considered have a wide range of microstructures, (typical crystallites are between 1 and 5 μm), the intermediate grained alumina with an average grain size of 9 μm and an alumina-based refractory with grog size of about 10^{-3} m. The experimentally obtained K_I - V data were fitted to straight lines to generate A and N as mentioned in Equation 8. Based on the microstructure, some values of D , S and θ are chosen.

3.1. Cordierite-based glass ceramics

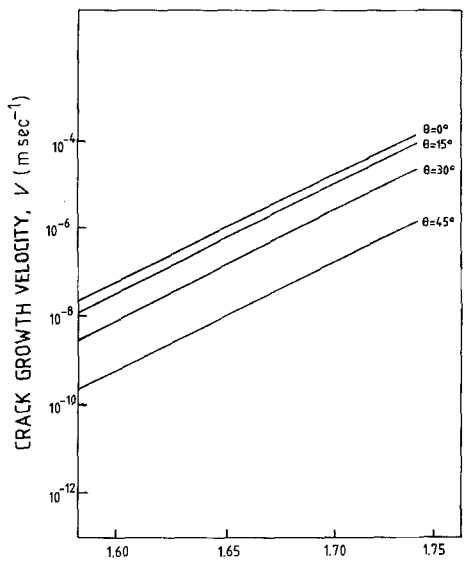
This material has been exclusively studied [13]. Basakaran *et al.* [14] also describe an interesting study of slow crack-growth data, fracture toughness data *vis-à-vis* the crystallite sizes produced by different heat treatments. The heat treatments typically include a nucleation heat treatment at 820°C for 2 h, followed by growth treatments at 1260°C for different periods of time. Table II lists these conditions, together with the fitted values for A and N . Although several scanning electron micrographs and fractographs are given [14], no crack path is shown. In the absence of an actual crack path, we have to choose a proper

TABLE II Subcritical crack growth parameters for cordierite glass ceramics, heat treated at 1260°C for various times

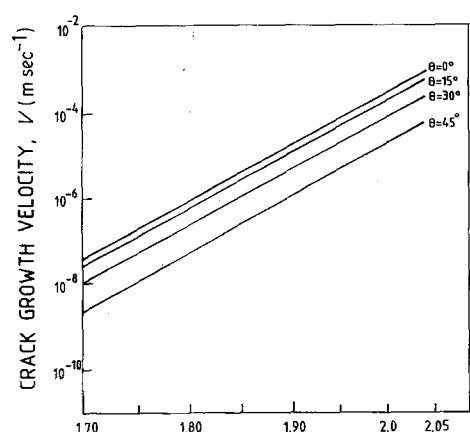
Heat treatment duration (h)	Fracture toughness (MPa m ^{1/2})	A	N
0.25	2.11	2.72×10^{-25}	98.90
1	2.20	1.53×10^{-27}	95.80
8	2.25	1.53×10^{-27}	55.80
24	2.52	2.02×10^{-27}	65.03
72	2.16	3.87×10^{-31}	112.00



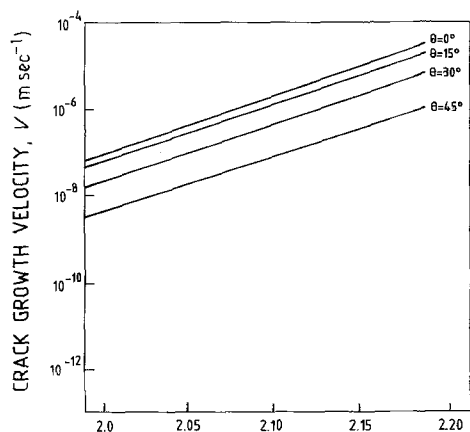
(a) STRESS INTENSITY FACTOR, K_I (MPa m^{1/2})



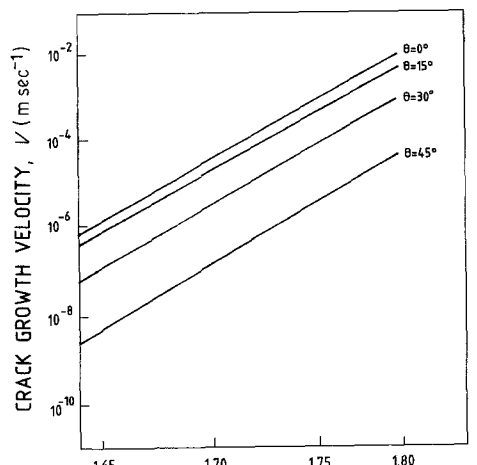
(b) STRESS INTENSITY FACTOR, K_I (MPa m^{1/2})



(c) STRESS INTENSITY FACTOR, K_I (MPa m^{1/2})



(d) STRESS INTENSITY FACTOR, K_I (MPa m^{1/2})



(e) STRESS INTENSITY FACTOR, K_I (MPa m^{1/2})

Figure 3 K_I - V data for cordierite-based glasses heat treated at 1260°C for (a) 15 min, (b) 1 h, (c) 8 h, (d) 24 h and (e) 72 h. Deflection condition: $D/(D + S) = 1/3$.

$D/(D + S)$ ratio. Initially, $D/(D + S)$ is chosen as 1/3 and θ is varied between 0° and 45° in the steps of 15°. Angles more than 45° seem to be improbable because they lead to an unusually high scatter in data. Figs 3a to e show the modified K_I - V curves for heat treatments at 1260°C for 15 min, 1, 8, 24 and 72 h, respectively.

3.2. Intermediate grain-sized alumina

The data for this material are taken from Pletka and

Wiederhorn [3]. In terms of the microstructure, this material has uniform grains as opposed to the previous material which, in fact, is a glass crystal composite. The intermediate grain-sized alumina has somewhat coarser grain size (average grain size $\approx 9 \mu\text{m}$) as compared to the previous material. Thus this material presents a microstructure of intermediate size. Fig. 4 shows the K_I - V curve for $D/(D + S) = 1/3$ and $\theta = 0^\circ, 15^\circ, 30^\circ, 45^\circ$. These graphs were plotted using $N = 99.1$ and $A = 1.48 \times 10^{-62}$.

3.3. Alumina refractories

This material represents the microstructure with coarse heterogeneities with grog sizes $\sim 1 \text{ mm}$ [15]. Fig. 5 shows the K_I - V data for $D/(D + S) = 1/3$ and $\theta = 0^\circ, 15^\circ, 30^\circ$ and 45° . N is assumed to be 69.4 and A is equal to 2.38×10^{-9} .

4. Discussion

4.1. Crack growth in heterogeneous materials compared to homogeneous materials

The model considers growth of large cracks in heterogeneous materials. Heterogeneities are supposed to

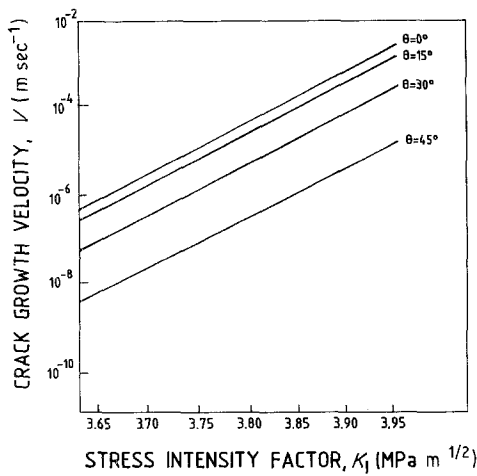


Figure 4 K_I - V data for intermediate grain-sized ($9\ \mu\text{m}$) alumina. Deflection condition: $D/(D + S) = 1/3$.

promote the so-called crack growth by deflection. Compared to heterogeneous materials, the crack growth occurs in a straight line fashion in a homogeneous material. Precisely for the same reason, there will be no difference in crack growth behaviour in large and small cracks. This leads to similar values of N , as determined from specimens with large cracks and those with short cracks. This conjecture is proved to be true in the case of ultra-low expansion glass, as reported by Pletka and Wiederhorn [3].

4.2. Effect of varying $D/(D + S)$ ratio and θ

So far we have only presented results with constant $D/(D + S)$ ratio and varying the angles of deflection. Fig. 6 shows a typical plot for intermediate grain-sized microstructure with $\theta = 30^\circ$ and $D/(D + S) = 0, 1/2, 1/3, 1/4, 1/5$ and values of A and N are chosen to be the same as those used for Fig. 4. It is observed from the plots that, with constant $D/(D + S)$ and increasing angles of deflection, the K_I - V curves shift to lower velocity values for the same K_I . The effect is the same when the extent of deflection $D/(D + S)$ is increased, keeping θ constant. Both the effects can be rationalized by using Equation 8. Physically speaking, the former case occurs when the heterogeneities are of uniform size and closely spaced. This is so in the cases of glass ceramics as well as intermediate grain-sized alumina and the alumina refractories. On the other

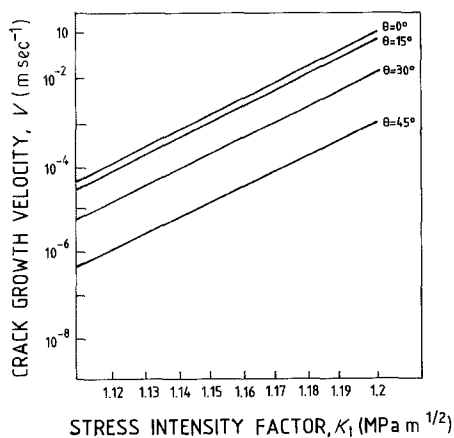


Figure 5 K_I - V data for the high alumina refractory. Deflection condition: $D/(D + S) = 1/3$.

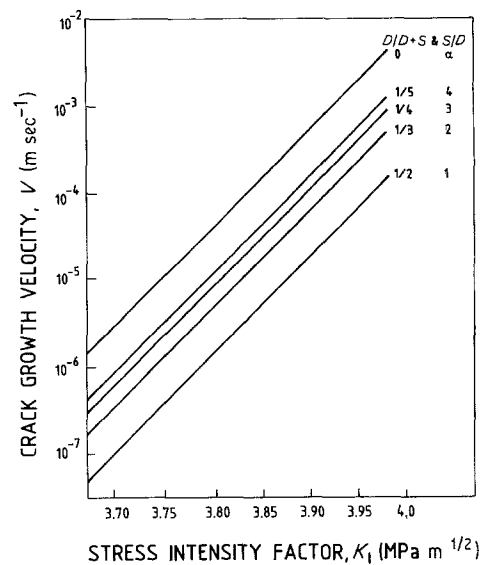


Figure 6 Effect of varying $D/(D + S)$ ratio on K_I - V data. Intermediate grain-size ($9\ \mu\text{m}$) alumina; deflection condition: $\theta = 30^\circ$.

hand, deflection at constant angle with varying $D/(D + S)$ may not occur in a physical system. However, even in a physically occurring system, crack growth may not be as simple as we have modelled but rather a mixture of both of the processes. So the parameters, $D/(D + S)$ and θ will change continuously as the crack is deflected by the microstructure.

We suggest, henceforth, one should be careful in obtaining crack-growth data for heterogeneous materials. Much attention must be paid to the actual crack path. From the crack paths the average values of $D/(D + S)$ and θ values should be calculated taking into consideration all the deflections that occurred during the crack growth. This kind of averaging procedure has been carried out by Faber and Evans [10].

4.3. Test technique and crack deflection

This topic can be sub-divided between specimens with long cracks and those with short cracks. As noted in Section 1, long cracks can be defined as those that geometrically extend through several heterogeneities. Short cracks, on the other hand, have dimensions the same as those of the heterogeneities. One reason why the N values from two types of specimens are different is argued to be the deflection of longer cracks around microstructures. However, Freiman *et al.* [16], have shown that in constant-moment DCB specimens, N values obtained are similar to those obtained from the stressing rate experiments. The reason for this is that in constant moment specimens, the crack is under constant driving force as opposed to the relaxation specimens where the driving force decreases as the crack grows. Constant driving force lets the crack propagate through the heterogeneities, though at a reduced speed. In relaxation experiments, the crack does not have that much driving force, especially towards the end of the relaxation. Thus, even though the crack is straight in the beginning of relaxation, it may deflect substantially at the end of the relaxation. Therefore, the crack-deflection model can be actually applied to DT relaxation data, where the propensity

for crack deflection is greater. In the present paper, data were selected involving DT load relaxation tests only; hence, the justification of applying the model to these cases.

In samples with short cracks, the interaction of the heterogeneities with the crack is much less. This is due to the nature of growth of the short crack. Because the short cracks have less energy, they usually stop when they encounter a tough heterogeneity. Another crack then starts growing instead.

4.4. Relationship between N and microstructure

We now discuss how the deflection crack growth can lead to an increase in N value in specimens having long cracks. Fig. 7 shows the K_I - V curves of glass ceramics heat treated at 1260°C for 8 h. The reason for choosing this material is because this is the commercial heat treatment. The conditions used here are $D/(D + S) = 1/3$ and $\theta = 0^\circ, 6^\circ, 12^\circ, 18^\circ, 24^\circ$ and 30° . Because of crack deflection, the actual K_I - V curve will

be somewhere in between. In a typical DT load relaxation test, the crack has a higher driving force in the beginning. So the probability of undergoing deflection is less and the crack will not initially deflect. On the other hand, deflection should be greater towards the end of the experiment (i.e. lower crack velocity and K_I). Crack path microstructures presented by Pletka and Wiederhorn [3] do not reveal much regarding this postulate. However, the SEM fractographs of glass ceramics presented by Baskaran *et al.* [14] clearly show that at lower K_I and V values, the crack has undergone deflection. We now assume the crack fol-

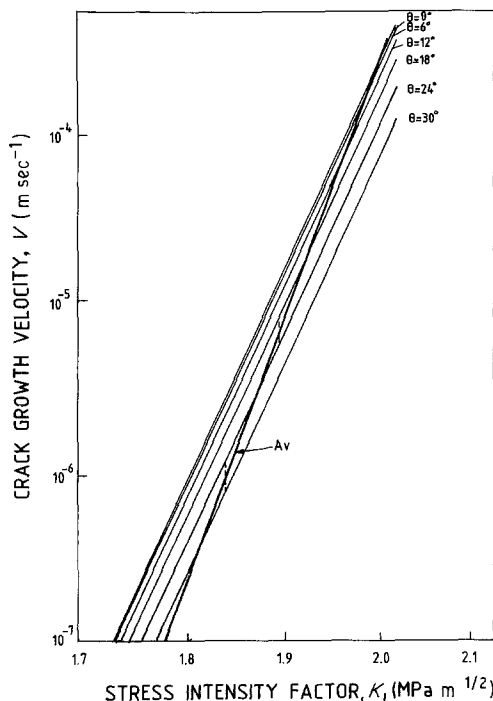


Figure 7 Simulation of actual crack deflection growth to show increase in N , for intermediate grain-sized ($9 \mu\text{m}$) alumina; deflection condition: $D/(D + S) = 1/3$.

lows a certain K_I - V curve and then due to deflection there is a sudden transition to a lower curve. The tendency will increase as we go down. The solid curve in Fig. 7 depicts this hypothetical curve and N is calculated to be 67.8.

4.5. Life-time prediction

The consequence of crack deflection is the change in life time of the structure. To determine life time, we consider the following equation

$$K_I = \sigma_a Y a^{1/2} \quad (9)$$

where K_I is the applied stress intensity factor, σ_a is the applied stress, Y is a geometrical constant and a is the flaw size. By differentiating Equation 8 with respect to time,

$$\frac{dK_I}{dt} = \left[\frac{(\sigma_a Y)^2}{2 K_I} \right] V \quad (10)$$

Substituting the crack-growth relationships of Equation 8 and integrating, we have

$$t_f = \frac{2[K_I^{2-N} - K_{Ic}^{2-N}]}{(\sigma_a Y)^2 \left[\frac{D \cos \theta + S}{(D + S)} \right]^{-1} \left[\frac{D \cos^2 \theta / 2 + S}{(D + S)} \right]^N A(N - 2)} \quad (11)$$

In Equation 11, the crack deflection effect is introduced by the factor

$$\left[\frac{D \cos \theta + S}{(D + S)} \right] \left[\frac{D \cos^2 \theta / 2 + S}{(D + S)} \right]^{-N}$$

Assuming $2D = S$ and N is the value of commercially heat-treated material, the above quantity is calculated to be 1.37, 3.49 and 15.973 for deflection angles $\theta = 15^\circ, 30^\circ$, and 45° , respectively, thus reflecting increase in life time due to crack deflection. Perhaps, it is not out of the way to point out that short cracks behave differently. As discussed by Okada and Sines [7], the short cracks propagate catastrophically. The life time consists of the time of growth of short cracks according to microscopic law, followed by the time of growth of a large coalesced crack according to the macroscopic law [7]. A particular situation will control which of the aforesaid processes is the deciding factor. It is shown in the example in [7] that both of the processes are important. Thus, in the growth of large cracks, deflection is important, whereas in case of small flaws, growth and coalescence are important.

In view of the above discussion, it is noted that life-time prediction using DT relaxation experiments may lead to higher prediction because the mode of crack growth will be different than what happens in a real situation.

4.6. Crack deflection compared to other mechanisms

Throughout this paper we have emphasized the fact that long cracks grow by deflection. However, it is worth noting that in some ceramic materials resistance to crack growth increases with the growth of the cracks [17-19]. This is known as R -curve behaviour. This behaviour is seen during the growth of a short crack to a long crack [4-6] and also during the growth

of cracks in intermediate grain-sized alumina [20–22]. The second case is pertinent to the present discussion. Two mechanisms have been proposed for this behaviour: (1) a microcrack zone ahead of the crack tip [23]; (2) bridging of unbroken ligaments behind the crack tip [22, 24, 26].

We note that during subcritical crack growth testing, the extent of crack growth is 100% of the starting crack. This extent of crack growth also takes place during *R*-curve determination tests. Ligament bridging can explain *R*-curve behaviour. Therefore, it may be likely that ligament bridging is taking place in intermediate grain-sized alumina during slow crack growth. One should expect K_I -*V* data with higher slopes with high *N* values. However, more experiments and modelling are required to quantify this statement. Becher and Ferber [25] argued that subcritical crack growth is affected by the residual grain-boundary stresses which are dependent on the grain size. However, if the grain size is greater than the critical grain size for microcracking, shielding of crack tip stresses occurs leading to an almost constant *N* value. Thus microcracking does not explain the observed results *per se*. For glass ceramics, there are no reported data on *R*-curve behaviour, so the present data can be explained only in terms of crack deflection.

Finally, *R*-curve behaviour is an effect of non-linear behaviour at the crack tip [23]. During the initial period of crack growth, there is a small zone at the crack tip. Because in the present case, the K_I values are less than K_{IC} it can be assumed that the zone around the crack tip is small in size. Therefore, *R*-curve behaviour is expected to be small. Hence, the present model of crack deflection can now suitably explain the experimental data.

5. Conclusions

This paper focuses on the behaviour of long cracks in heterogeneous ceramics. From the microstructures of crack paths presented in the literature, it was concluded that the crack undergoes deflection during subcritical crack growth. Two most important crack-deflection configurations are tilt and twist modes. In the present model, a simplifying assumption was made by considering only the tilt mode. Calculations show deflection causes substantial scatter in K_I -*V* data and predict a systematic shift of *N* towards higher values. The above conclusion is true for heterogeneities of different sizes (10^{-6} to 10^{-3} m). It is shown that data taken from DT relaxation experiments will lead to a higher predicted life time.

Acknowledgement

The authors thank Dr P. Rama Rao, Director, Defence Metallurgical Research Laboratory, for his encouragement and permission to publish this paper.

References

1. S. M. WIEDERHORN, in "Fracture Mechanics of Ceramics", Vol. 2, edited by R. C. Bradt, F. F. Lange and D. P. H. Hasselman (Plenum, New York, 1974) p. 613.
2. B. J. PLETKA and S. M. WIEDERHORN, *ibid.* Vol. 4, (1978) p. 745.
3. *Idem*, *J. Mater. Sci.* **17** (1982) 1247.
4. R. F. COOK, B. R. LAWN and C. J. FAIRBANKS, *J. Amer. Ceram. Soc.* **68** (1985) 604.
5. *Idem*, *ibid.* **68** (1985) 616.
6. B. R. LAWN, S. W. FREIMAN, T. L. BAKER, D. D. COBB and A. C. GONZALES, *ibid.* **67** (1984) C-67.
7. T. OKADA and G. SINES, *ibid.* **66** (1983) 719.
8. B. G. KOEPKE, K. D. McHENRY and W. D. SAVAGE, *Bull. Amer. Ceram. Soc.* **58** (1978) 1100.
9. J. G. BRUCE, W. H. GERBERICH and B. G. KOEPKE, in "Fracture Mechanics of Ceramics", Vol. 4, edited by R. C. Bradt, F. F. Lange and D. P. H. Hasselman (Plenum, New York, 1978) p. 687.
10. K. T. FABER and A. G. EVANS, *Acta Metall.* **31** (1983) 565.
11. S. SURESH, *Met. Trans.* **14A** (1983) 2375.
12. B. R. LAWN and T. R. WILSHAW, in "Fracture Mechanics of Brittle Solids" (Cambridge University Press, Cambridge, 1975) p. 67.
13. G. K. BANSAL and W. H. DUCKWORTH, *J. Mater. Sci.* **13** (1978) 239.
14. S. BASKARAN, S. B. BHADURI and D. P. H. HASSELMAN, *J. Amer. Ceram. Soc.* **68** (1985) 112.
15. T. E. ADAMS, D. J. LANDINI, C. A. SCHUMACHER and R. C. BRADT, *Bull. Amer. Ceram. Soc.* **60** (1981) 730.
16. S. W. FREIMAN, K. R. McKINNEY and H. L. SMITH, in "Fracture Mechanics of Ceramics", Vol. 2, edited by R. C. Bradt, F. F. Lange and D. P. H. Hasselman (Plenum, New York, 1974) p. 659.
17. H. HUBNER and W. JILLEK, *J. Mater. Sci.* **12** (1977) 117.
18. M. V. SWAIN and R. H. J. HANNINK, in "Advances in Ceramics", Vol. 12, edited by N. Claussen, M. Ruhle and A. H. Heuer (American Ceramic Society, Columbus, Ohio, 1984) p. 225.
19. G. HIMMOLT, H. KNOCH, H. HUBNER and F. W. KLEINLEIN, *J. Amer. Ceram. Soc.* **62** (1973) 485.
20. R. KNEHANS and R. STEINBRECH, *J. Mater. Sci. Lett.* **1** (1982) 327.
21. R. STEINBRECH, R. KNEHANS and W. SCHAARWACHTER, *J. Mater. Sci.* **18** (1983) 265.
22. M. V. SWAIN, *J. Mater. Sci. Lett.* **5** (1986) 1313.
23. A. G. EVANS, in "Advances in Ceramics", Vol. 12, edited by N. Claussen, M. Ruhle and A. H. Heuer (American Ceramic Society, Columbus, Ohio 1984) p. 193.
24. C. FAIRBANKS, B. R. LAWN, R. F. COOK and Y-W. MAI, in "Fracture Mechanics of Ceramics", Vol. 8, edited by R. C. Bradt, A. G. Evans, D. P. H. Hasselman and F. F. Lange (Plenum Press, New York, 1986) p. 23.
25. P. F. BECHER and M. K. FERBER, *Acta Metall.* **33** (1985) 1217.
26. Y-W. MAI and B. R. LAWN, *J. Amer. Ceram. Soc.* **70** (1987) 289.

Received 15 May
and accepted 16 May 1987